Journal of Solid State Chemistry 182 (2009) 1021–1026

Contents lists available at ScienceDirect

Journal of Solid State Chemistry

journal homepage: www.elsevier.com/locate/jssc

A fast route to obtain manganese spinel nanoparticles by reduction of K-birnessite

F. Giovannelli [a,*], T. Chartier [a], C. Autret-Lambert [b], F. Delorme [c,d], M. Zaghrioui [a], A. Seron [c]

[a] LEMA, UMR 6157 CNRS-CEA, Université François Rabelais, 3 place Jean Jaurès 41029 BLOIS, France
[b] LEMA, UMR 6157 CNRS-CEA, Université François Rabelais, parc de Grandmont 37200 TOURS, France
[c] BRGM, 3 Avenue Claude Guillemin, BP 36009, 45060 ORLEANS Cedex 2, France
[d] CORNING SAS, CETC, 7 bis Avenue Valvins, 77210 AVON, France

ARTICLE INFO

Article history:
Received 26 August 2008
Received in revised form
19 December 2008
Accepted 26 January 2009
Available online 5 February 2009

Keywords:
Nanoparticles
Birnessite
Hausmanite
Reduction
Spinel

ABSTRACT

The K-birnessite ($K_xMnO_2 \cdot yH_2O$) reduction reaction has been tested in order to obtain manganese spinel nanoparticles. The addition of 0.25 weight percent of hydrazine hydrate, the reducing agent, during 24 hours is efficient to transform the birnessite powder in a hausmanite Mn_3O_4 powder. Well crystallised square shape nanoparticles are obtained. Different birnessite precursors have been tested and the reaction kinetics is strongly correlated to the crystallinity and granulometry of the precursor. The effects of aging time and hydrazine hydrate amount have been studied. Well crystallised Mn_3O_4 is obtained in one hour. The presence of feitknechtite (MnO(OH)) and amorphous nanorods has been detected as an intermediate phase during birnessite conversion into hausmanite. The conversion mechanism is discussed.

1. Introduction

Manganese oxides have focussed attention due to their numerous potential applications and their low cost. Manganites presenting Colossal Magneto Resistance properties are, for example, considered in microelectronic devices [1,2]. Electrochemical properties of layered manganese oxides are also attractive for cathodic materials in lithium batteries [3,4]. Moreover, catalytic activity of spinel Mn_3O_4 (hausmanite) towards NO_x or cyclohexane is of potential interest [5,6]. For this kind of application, a high specific surface area is required which can be attained by synthesis of Mn_3O_4 powder of nanometre size.

Recently, different routes to obtain Mn_3O_4 nanopowders have been proposed. Mn_3O_4 is often synthesised by high temperature treatment ($T > 900\,^{\circ}C$) which implies grain coarsening. Different soft chemistry processes have been reported in order to decrease the temperature and the grain size, and consequently to lower the cost of the synthesis and to increase the powder reactivity. Synthesis of Mn_3O_4 in microwave reactor allows obtaining of nanopowders at about $100\,^{\circ}C$ [7–9]. At similar temperature ($80\,^{\circ}C$), solvothermal method, which implies an organic solvent, is also efficient to obtain hausmanite nanocrystals [10]. At room temperature, Vasquez-Olmos et al. [11] have reported the synthesis of Mn_3O_4 nanorods via a three month-long sol–gel route. A faster method consists in an ultrasonic treatment during 3 hours of an aqueous manganese acetate solution [12].

Several studies have also shown the possible conversion of a manganese compound in another structure. For example, Folch et al. [13] have converted MnOOH nanorods into Mn_3O_4 or MnO_2 nanorods by calcinations at $400\,^{\circ}C$. The inverse conversion has been observed by Lind [14] in dilute oxalate solution. Ferreira et al. [15] have prepared MnO(OH) nanorods from platelike birnessite, $Na_{0.33}MnO_2 \cdot xH_2O$, by hydrothermal treatment at low temperature, $170\,^{\circ}C$ during 120 hours. Mn_2O_3 and Mn_3O_4 have been prepared by oxidation of $Mn(OH)_2$ [6]. The numerous oxidation states of manganese allow considering oxidation or reduction reactions as a mean for converting manganese compounds. Sometimes this transformation is a disadvantage for application. For example, the reduction of manganese dioxide electrodes leads to different structures during redox processes. Indeed, the spinel structure (manganese average valence is 2.66) appeared after repeated discharge–recharge cycles on lamellar $LiMnO_2$ which has been tested as cathode in Li secondary batteries [16]. In the case of pure MnO_2 (Mn^{4+}) the reduction to MnOOH (Mn^{3+}) is reported in a first step and to MnO (Mn^{2+}) in a second step [17]. So the reduction of lamellar MnO_2 leads to different manganese oxides or hydroxides.

In this paper, a fast and simple route to Mn_3O_4 nanopowders synthesis is reported. The effect of hydrazine hydrate on K-birnessite ($K_xMnO_2 \cdot yH_2O$) has been tested at room temperature

* Corresponding author. Fax: +33 2 54 55 21 37.
E-mail address: fabien.giovannelli@univ-tours.fr (F. Giovannelli).

0022-4596/$ - see front matter © 2009 Elsevier Inc. All rights reserved.
doi:10.1016/j.jssc.2009.01.031

and atmospheric pressure. The hydrazine hydrate has been chosen as reducing agent. The influence on the process of hydrazine hydrate proportion, time and K-birnessite crystallinity and granulometry, has been observed.

2. Experimental

The K-birnessite precursors have been processed by two different routes. The first one is a sol–gel process which consists in the reduction of $KMnO_4$ by sugars [18]. The obtained gel is dried under vacuum and then heated at 400 °C during 2 hours. This route allows obtaining submicronic grains, is called birn400 in the following sections. The second one consists in the pyrolysis of $KMnO_4$ at 800 °C [4]. After decomposition, the soluble by-products (K_3MnO_4 and K_2MnO_4) are removed by washing in distilled water until disappearing of the purple colour of water. The suspension is then filtered and the resulting powderdried at 80 °C, and is called birn800.

The K-birnessite, synthesised by these two different methods, is used as precursor in order to obtain hausmanite. For each experiment, 0.5 g of birnessite is added under vigorous stirring in different reducing solutions. Hydrazine hydrate (98% Lancaster) is dissolved in 75 ml of deionised water. The stoechiometric reduction reaction of birnessite corresponds to a hydrazine hydrate amount of 0.15 weight percent. The influence of hydrazine quantity and aging time has been tested: 0.25, 0.15 and 0.1 weight percent of hydrazine hydrate have been added. The solution is filtered after 15 minutes, one hour or 24 hours and the resulting powder is then washed in deionised water and dried under vacuum.

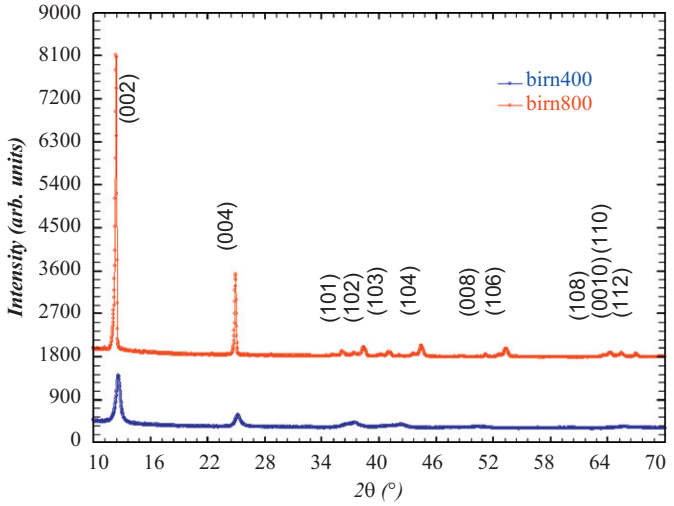

Fig. 1. X-ray diffraction pattern of: (A) birn800 and (B) birn400.

The powder X-ray diffraction patterns of all samples were collected at room temperature using Rigaku diffractometer in a θ–2θ geometry over a 2θ angular range of 10°–120° with a step of 0.02° and a time per step of 10 seconds. Cu $K\alpha$ radiation was employed, with a tube current of 15 mA and a tube voltage of 30 KV. The data were analysed with the Rietveld method using FULLPROF program [19].

Scanning electron microscopy observations were performed with a Quanta 200 microscope (FEI) at 5 KV. The samples were previously sputter-coated with a thin film of gold. All the images were realised with secondary electrons.

The specific surface area was determined from the nitrogen adsorption isotherm at 77 K treated according to the BET method. Prior to the measurement, the sample was outgassed at 110 °C for 72 hours. At the end of the outgassing process, the residual pressure was below 0.05 mbar. The measurement has been realised in a multipoint adsorptometer Micromeritics Tristar 3000.

Transmission electron microscopy samples were prepared by crushing the agglomerates in n-butanol and the small crystallites in suspension were deposited on a holey carbon film, supported by a copper grid. The electron diffraction and the high resolution electron microscopy were performed with a JEOL 2100F electron microscope equipped with a tilting and rotating goniometer (200 kV and point resolution of 1.8 Å).

3. Results and discussion

3.1. Effect of precursor

Birn400 and birn800 samples exhibit layered MnO_2 structure (Fig. 1). The powders only show the diffraction lines of birnessite, in agreement with JCPDS 43-1456, without impurities. As already reported by Kim et al. [4], the higher thermal treatment improves the X-ray diffraction pattern (Fig. 1A). Indeed, birn800 exhibits platelike grains of few microns (Fig. 2A). The shape of grains is correlated to lamellar structure of birnessite which induces an anisotropic growth rate. The sol–gel process, birn400, leads to agglomerated submicronics grains (Fig. 2B). The X-rays pattern

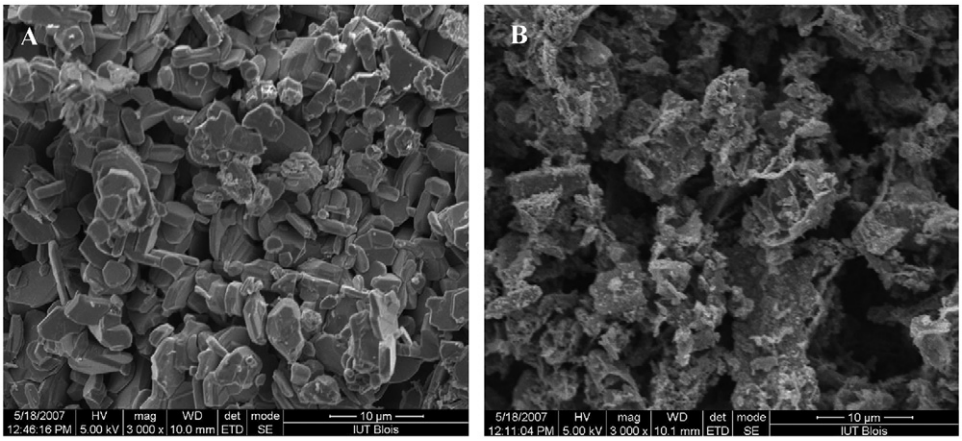

Fig. 2. SEM images showing: (A) birn800 and (B) birn400.

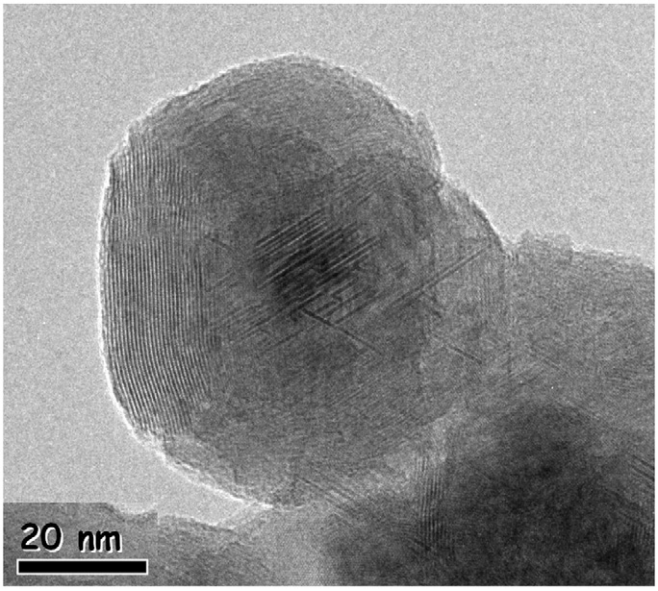

Fig. 3. TEM image showing birn400.

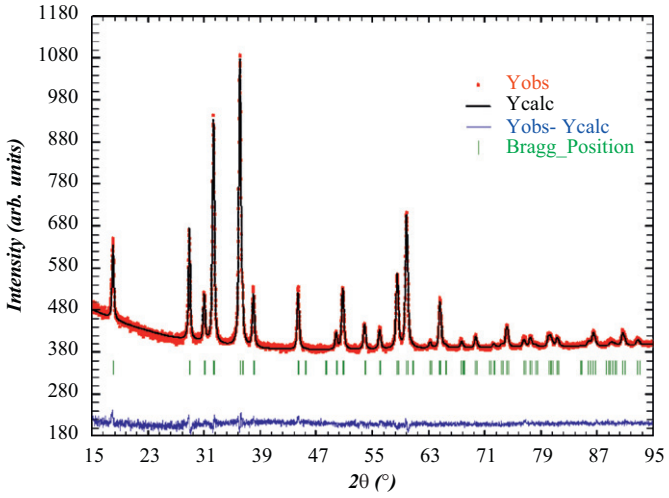

Fig. 4. X-ray diffraction pattern of birn400 after treatment with an addition of 0.25 weight percent of hydrazine during 24 hours.

peaks are larger and less well defined than in the case of birn800 (Fig. 1B). Moreover, a slight shift of (00l) peaks is observed. For example, the position of (002) peak is 12.61° 2θ in birn400 in comparison of 12°43 2θ in birn800. This shift is due to the thermal treatment at 800 °C which induces a dehydratation of interlamellar space. The TEM observation of birn400 shows the nanometric size of the particles, about 50 nanometres diameter (Fig. 3). Each particle is divided in subgrains which imply a low coherence length. Therefore, the broadening of the XRD pattern peaks in the sol–gel process is attributed to the finite-size of the small particles and their low coherence length.

These two morphologies of grains allow to change the specific surface area of the precursor and to test its influence on the reduction process.

In the first test, the process time has been fixed at 24 hours and an excess of hydrazine has been added (0.25 weight percent) in comparison with stoechiometric reaction requirements (0.15 weight percent). Rietveld analyses have been performed on the resulted powder, using birn400 as precursor. The powder exhibits the hausmanite structure with an *I*41/*amd* space group (JCPDS 24-0734), and no impurity is detected (Fig. 4). So, the process is efficient to transform birnessite in Mn_3O_4 powder. The SEM image shows submicronic grains forming agglomerates (Fig. 5A). TEM image (Fig. 5B) exhibits nanometre size particles, with a well defined square shape. The crystallite edges are sharp and the atomic planes are periodic. Contrary to the precursor (birn400), the hausmanite particles are single crystallite with unique coherence length. No structural defect is observed. The particle size has been measured on 30 particles and an average size of 50 nanometres has been determined with a dispersion of 15 nanometres. The measured specific surface area is 30.7 $m^2 g^{-1}$.

In the same experimental conditions with the birn800, Fig. 6A shows agglomerates of submicronic particles. However, in the previous case the agglomerates have a spherical shape whereas with birn800 the agglomerates of small particles conserve the platelike shape of the precursor. In fact, two kinds of crystallites are present in the powders: in one hand, hausmanite with an average size of about 50 nanometres; and in other hand birnessite with a size higher than 100 nanometres (Fig. 6B). The X-ray pattern confirms the presence of hausmanite and birnessite (Fig. 7). A slight shift of birnessite (001) and (002) peaks, respectively, 12.5° 2θ and 25° 2θ, is also observed and could be linked to the hydratation of interlamellar space of birn800 during the process [19]. Moreover, a reflection is present at about 19° 2θ which could not be attributed to the birnessite or hausmanite

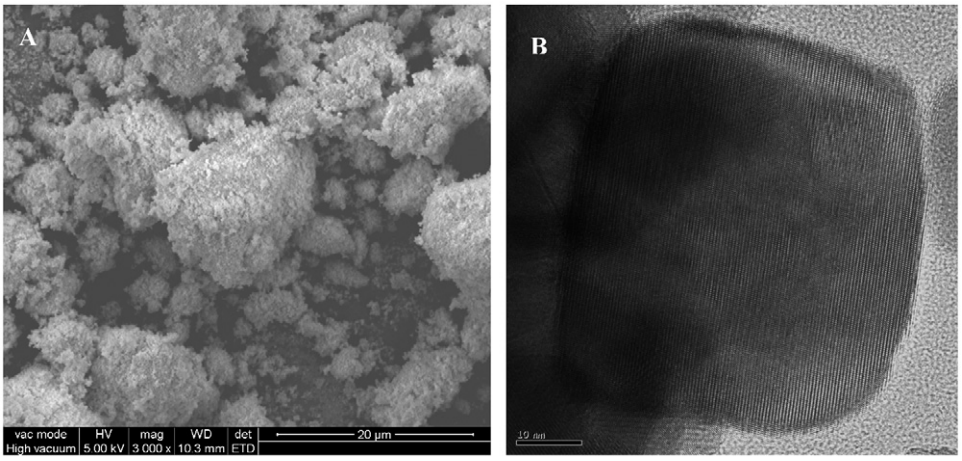

Fig. 5. SEM image (A) and TEM image (B) showing birn400 after treatment with an addition of 0.25 weight percent of hydrazine during 24 hours.

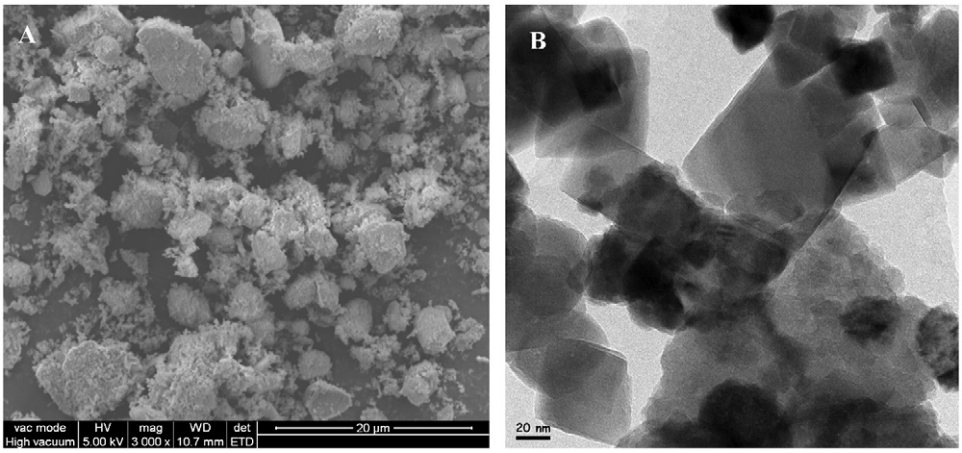

Fig. 6. SEM image (A) and TEM image (B) showing birn800 after treatment with an addition of 0.25 weight percent of hydrazine during 24 hours.

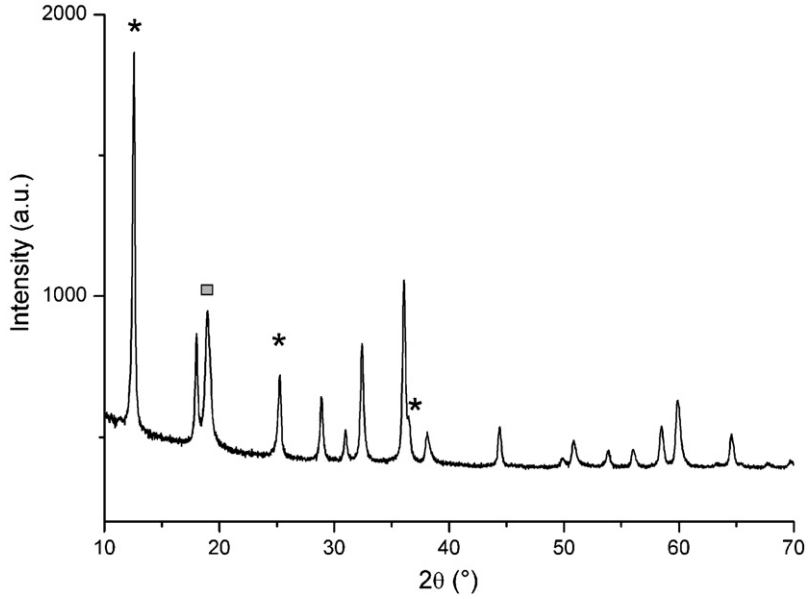

Fig. 7. X-ray diffraction pattern of birn800 after treatment with an addition of 0.25 weight percent of hydrazine during 24 hours: (∗) birnessite phase, (□) feitknechtite phase.

structure. This reflection could be attributed to the feitknechtite β-MnOOH phase (JCPDS 18-804), which could be an intermediate phase of the reduction of birnessite in hausmanite. Indeed, the oxidation degree of manganese in this structure (+3) is intermediate between birnessite (+4) and hausmanite (+2.66). In an aqueous system, the presence of feitkneichtite has been already reported by Luo et al. [20] as an intermediate phase during the oxidation of pyrochroite $Mn(OH)_2$ to birnessite. They have shown the progressive conversion of pyrochroite in feitkneichtite and then in birnessite versus the oxidising agent (H_2O_2) addition. Ferreira et al. [15] have proposed a reaction mechanism of sodium–birnessite ($Na_{0.33}MnO_2 \cdot xH_2O$) reduction in an autoclave by dodecylamine. They obtained γ-MnOOH with the presence of Mn_3O_4. In a first step, Na^+ ion of birnessite are partially exchange during 48 hours by $C_{12}H_{25}$–NH_3^+ cation due to protonation of dodecylamine. The intercalation phenomenon leads to an increase of interlayer distance. The reduction process is initiated by an autoclave treatment. This reaction mechanism could describe the effect of hydrazine. Indeed, hydrazine is probably protonated ($N_2H_4+H^+ \rightarrow N_2H_5^+$) and then intercalated in birnessite. The first

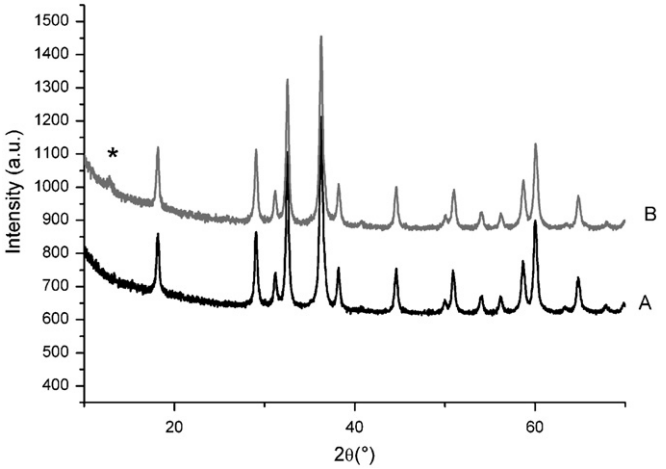

Fig. 8. X-ray diffraction pattern of birn400 after treatment with an addition of 0.25 weight percent of hydrazine versus of aging time: one hour (A), 15 minutes (B) ((∗) birnessite phase).

step of mechanism for the birnessite transformation leads to a N_2H_5 $MnO_2 \cdot xH_2O$ intermediate phase. According to the crystallinity and particles size of birnessite, the kinetic of the reaction change. The second step of the reaction is the reduction of birnessite by hydrazine following the reaction:

$$3MnO_2 + N_2H_5^+ \rightarrow Mn_3O_4 + N_2 + 2H_2O + H^+$$

As hydrazine has a high reducing power, the kinetics of the second step of the transformation is fast. It is the reason why the $N_2H_5 \cdot MnO_2 \cdot xH_2O$ intermediate phase could not be observed in XRD pattern. This fast kinetic is confirmed by the observation of effervescence after birnessite addition to hydrazine reducing solution. Indeed, the oxidation of hydrazine leads to N_2 liberation. Moreover, the reducing power of hydrazine is higher than dodecylamine one, leading to the birnessite transformation to hausmanite and not to γ-MnOOH. The kinetics of the total reaction appears as strongly correlated to precursor's low coherence length. As the birn400 is more reactive than birn800, it will be use as the precursor used in the following tests.

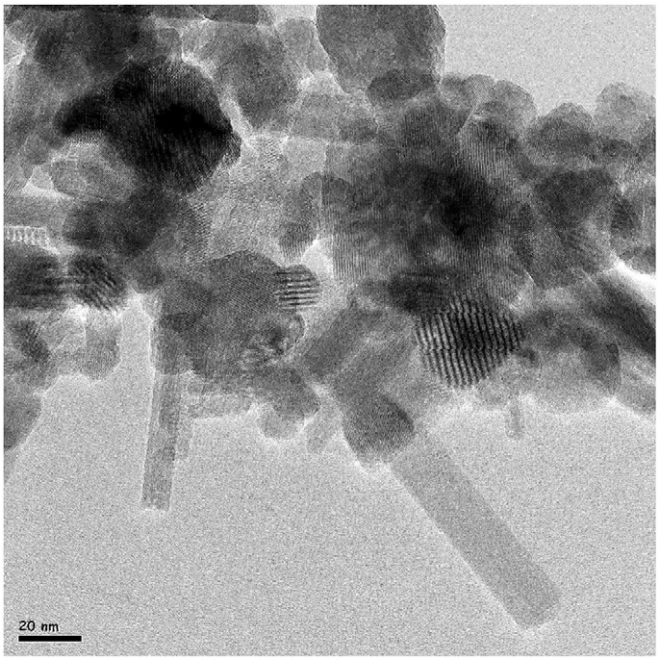

Fig. 9. TEM image of birn400 after treatment with an addition of 0.25 weight percent of hydrazine during 15 minutes

3.2. Effect of time and hydrazine rate

In order to observe the reaction kinetics, the aging time has been decreased with a hydrazine addition of 0.25 weight percent. One hour aged powder only shows the diffraction lines of well crystallised hausmanite (Fig. 8A). In the case of an aging time of 15 minutes, a 12.88°2θ small supplementary peak is detected on the diffraction pattern (Fig. 8B). This peak could be attributed to the birnessite precursor which shows that the reaction is not complete. TEM observations of 15 minutes aged powder show the presence of amorphous nanorods (Fig. 9). Their size could reach more than 100 nanometres with a diameter of 10 nanometres. An aging time of one hour is necessary to observe the complete reaction.

The effect of initial amount of hydrazine on the reaction kinetic has been also studied. The test time has been fixed at 24 hours. If 0.15 weight percent of hydrazine is added to birn400, the hausmanite structure is still present. However, supplementary small peaks are observed at about 12°2θ and 24°2θ on X-ray pattern which could be attributed to birnessite (Fig. 10). A hydrazine amount of only 0.1% allows observing the same peaks. The presence of birnessite is therefore expected as the added amount of hydrazine is not enough for complete reaction. In the case of 0.15% hydrazine amount, the presence of birnessite means that an excess of hydrazine is necessary in order to complete the

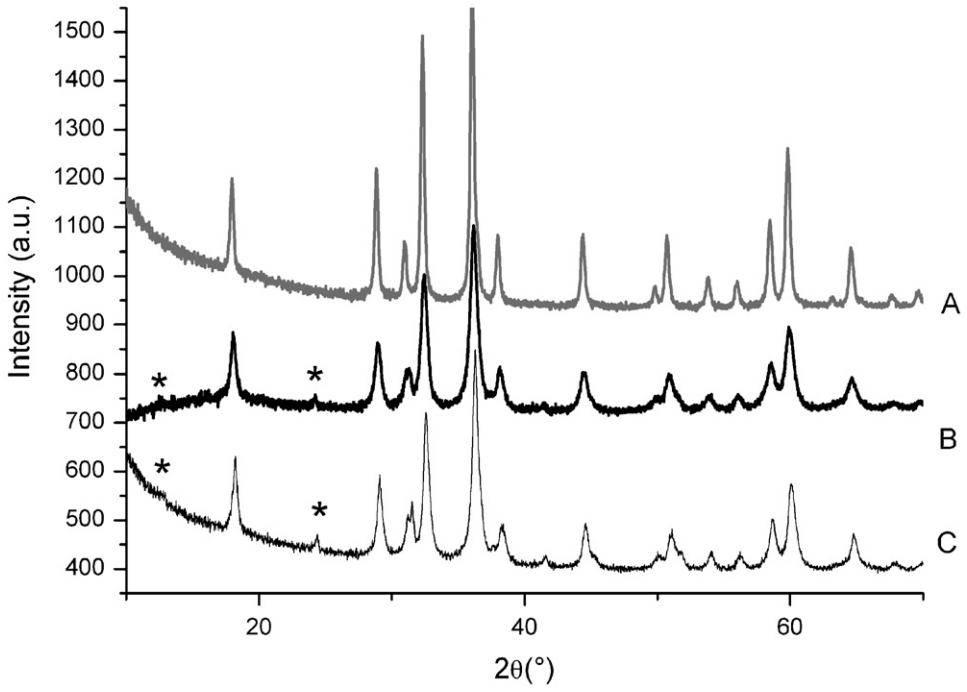

Fig. 10. X-ray diffraction pattern of birn400 after treatment by hydrazine during 24 hours versus weight percent hydrazine amount: 0.25% (A), 0.15% (B) and 0.1% (C) ((*) birnessite phase).

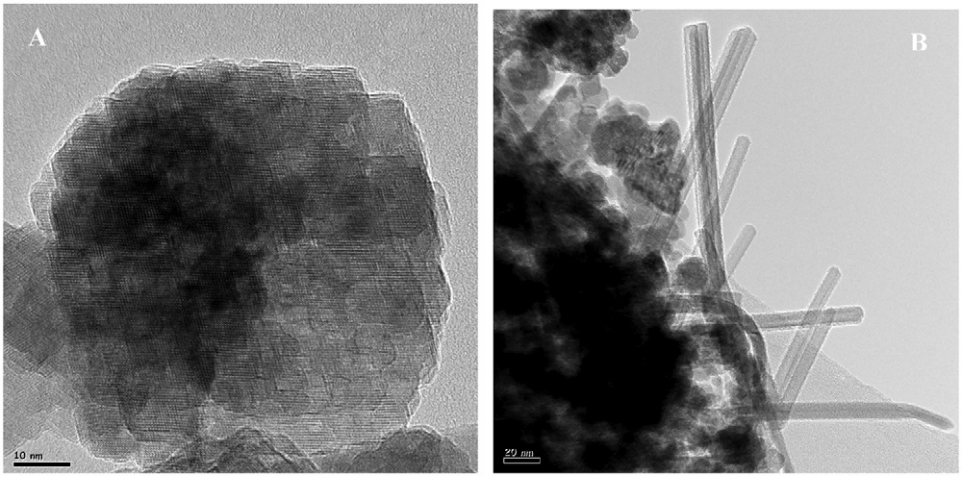

Fig. 11. TEM images showing birn400 after treatment with an addition of 0.1 weight percent of hydrazine during 24 hours.

reaction or that the kinetic is not fast enough. Moreover, when the hydrazine addition decreases, the X-ray pattern exhibits an increase of the full width middle high hausmanite peaks in comparison with the 0.25 weight percent of hydrazine addition. This could be correlated to a hausmanite particles coherence length decrease. TEM analyses confirm this hypothesis (Fig. 11A). The hausmanite particles size is about 50 nanometres as for the complete reaction (Fig. 5B). However, each particle is an agglomerate of small grains with different crystallographic orientation which imply a low coherence length. Amorphous nanorods are observed when the hydrazine addition decreases (Fig. 11B). Their presence is important for 0.1 weight percent hydrazine rate. In the case of 0.15 weight percent hydrazine addition, only few nanorods are detected. When the reaction is not complete, with birn400 precursor, amorphous nanorods are always detected. These particles are an intermediate phase in the birnessite reduction reaction. However, with birn800 precursor, these particles are not detected whereas the reaction is not complete. In this case, feitknechtite is present on diffraction pattern (Fig. 1C). The intermediate phase thus seems to depend on the cristallinity of the precursors.

Whatever the precursors, the hausmanite particles exhibit a different size and morphology than the birnessite. The conversion reaction leads to an intermediate phase which could be feitknechtite or amorphous rod. These amorphous rods could reach a size higher than 100 nanometres. All these observations indicate that the reaction is not topotatical.

4. Conclusion

An easy and fast route has been developed to obtain hausmanite nanoparticles. Indeed, the hydrazine hydrate reduces birnessite and allows crystallising 50 nanometres square shape hausmanite particles. Two kind of birnessite precursor, one nanometric and one micrometric, have been tested which influences the kinetic and the intermediate phase of the reaction. The first step of phase transformation is an intercalation of hydrazine in the birnessite and the second step is a reduction of manganese leading to the spinel structure. A decrease of hydrazine hydrate addition does not allow the complete reaction and the presence of birnessite is detected with the presence of an intermediate phase. The nature of this intermediate phase depends on the nature of the K-birnessite precursor. The aging time could be decreased until one hour in order to synthesise pure hausmanite.

References

[1] C.N.R. Rao, B. Raveau (Eds.), Colossal magnetoresistance, charge ordering and related properties of manganese oxide, World Scientific, Singapore, 1998.
[2] A. Barthelemy, A. Fert, J.-P. Contour, M. Bowen, V. Cros, J.M. De Teresa, A. Hamzic, J.C. Faini, J.M. George, J. Grollier, F. Montaigne, F. Pailloux, F. Petroff, C. Vouille, Journal of Magnetism and Magnetic Materials 242–245 (2002) 68–76.
[3] J.M. Tarascon, M. Armand, Nature 414 (2001) 359–367.
[4] S.H. Kim, S.J. Kim, S.M. Oh, Chemistry of Materials 11 (1999) 557–563.
[5] T. Yamashita, A. Vannice, Journal of Catalysis 163 (1996) 158–168.
[6] Z.R. Tian, W. Tong, J.Y. Wang, N.G. Duan, V.V. Krishnan, S.L. Suib, Science 276 (1997) 926–930.
[7] C. Bousquet-Berthelin, D. Stuerga, Journal of Material Science Letters 40 (2005) 253–255.
[8] S.K. Apte, S.D. Naik, R.S. Sonawane, B.B. Kale, N. Pavaskar, A.B. Mandale, B.K. Das, Materials Research Bulletin 41 (2006) 647–654.
[9] L.X. Yang, Y.J. Zhu, H. Tong, W.W. Wang, G.F. Cheng, Journal of Solid State Chemistry 179 (2006) 1225–1229.
[10] W. Zhang, Z. Yang, Y. Liu, S. Tang, X. Han, M. Chen, Journal of Crystal Growth 263 (2004) 394–399.
[11] A. Vasquez-Olmos, R. Redon, A.L. Fernandez-Osorio, J.M. Saniger, Applied Physics A 81 (2005) 1131–1134.
[12] I.K. Gopalakrishnan, N. Bagkar, R. Ganguly, S.K. Kulshreshtha, Journal of Crystal Growth 280 (2005) 436–441.
[13] B. Folch, J. Larionova, Y. Guari, C. Guerin, C. Reibel, Journal of Solid State Chemistry 178 (2005) 2368–2375.
[14] C.J. Lind, Environmental Science & Technology 22 (1988) 62–70.
[15] O.P. Ferrreira, L. Otubo, R. Romano, O.L. Alves, Crystal Growth and Design 6 (2006) 601–606.
[16] G. Vitins, K. West, Journal of the Electrochemical Society 144 (1997) 2587–2592.
[17] S.W. Donne, G.A. Lawrance, D.A.J. Swinkels, Journal of the Electrochemical Society 144 (1997) 2949–2953.
[18] S. Ching, J.A. Landrigan, M.L. Jorgensen, N. Duan, S.L. Suib, Chemistry of Materials 7 (1995) 1604–1606.
[19] J. Rodriguez-Carvajal, FULLPROF: a program for Rietveld refinement and pattern matching analysis, Abstracts of the Satellite Meeting on Powder Diffraction of the XV Congress of the IUCr, Toulouse, France, 1990, p. 127.
[20] J. Luo, Q. Zhang, S.L. Suib, Inorganic Chemistry 39 (2000) 741–747.